

## Novel fast terminal sliding mode controller with current constraint for permanent-magnet synchronous motor

Yao FANG\*, Huifang KONG , Daoyuan DING 

School of Electrical Engineering and Automation, Hefei University of Technology, Hefei City, China

Received: 17.07.2020

Accepted/Published Online: 11.12.2020

Final Version: 31.05.2021

**Abstract:** Under the noncascade structure, the balance between q-axis current constraint and dynamic performance in permanent-magnet synchronous motor system has become a critical problem. On the one hand, large transient current is required to provide high torque to achieve fast dynamic performance. On the other hand, current constraint becomes a state constraint problem, instead of governing q-axis reference current in the cascade structure directly. Aiming at this issue, a novel fast terminal sliding mode control (FTSMC)-based controller with current constraint is developed in this paper. The novelty of this scheme is related to the proposed penalty function based on interior point method, which is established in control action directly. Unlike ordinary solutions, the suggested solution combined with sliding mode variable can achieve current constraint of q-axis without sacrificing dynamic performance. Furthermore, by adopting the FTSMC-type surface and new reaching law, the proposed implementation guarantees high performance with significant reduction of chattering phenomenon and has fast convergence characteristics. Then, the stability proof of the whole closed-loop system by employing the Lyapunov method is given in detail. Finally, series of simulations are provided to evaluate the performance of the presented FTSMC-type controller, in terms of current constraint, dynamic performance, and chattering reduction.

**Key words:** Permanent-magnet synchronous motor, current constraint, fast terminal sliding mode control, reaching law

### 1. Introduction

In real industrial applications, permanent-magnet synchronous motor (PMSM) as a powerful competent has been extensively investigated in applications of motion control system, due to its merits such as high-power density, low inertia, and high efficiency [1].

So far, field-orientation control (FOC) framework with two loops has been extensively used for PMSM control systems [2]. Under this framework, PI controllers of q-axis and d-axis are designed to allow a PMSM to perform as an excited DC motor [3]. It should be emphasized that conservative parameters should be selected to reduce system overshoot. It unavoidably leads to weakness in the antiinterference capability and dynamic performance of PMSM systems [4]. Moreover, PI controllers in cascade structure unavoidably affect the transient response and dynamic performance of PMSM systems [5]. In addition, the stability proof of two loops is given in detail, but the stability of the whole cascade system cannot be ensured [6]. Especially the difference of control frequency between two loops is becoming smaller and even disappeared along with technology development [7]. In such cases, various noncascade approaches with single-loop control structure are developed to overcome the

\*Correspondence: 13095518972@163.com

shortcomings of cascade control, e.g., modified backstepping control [8], passivity control [9], model predictive control (MPC) [10], and sliding mode control (SMC) [6], and the system performance is perfected in different aspects.

Constraint of overlarge current is a critical challenge in the noncascade structure [11]. Because inner loop and outer loop are integrated, the q-axis current becomes an internal variable instead of the reference signal of the q-axis controller. Therefore, the overcurrent protection becomes a state constraint problem rather than restricting the q-axis reference current in the cascade structure directly. Several modern schemes have been applied to PMSM systems with state constraint [12–15]. In [13], MPC-based PMSM controller with current constraint was developed to handle the control problem with state constraint. The mechanism of MPC controller is to produce the control variable by minimizing cost function which is constructed by weight of constrained states. It should be noted that computation burden of MPC limits the practical application in PMSM systems [15]. In recent years, backstepping approaches based on barrier Lyapunov function (BLF) have provided us with an alternative control method for the state-constrained control system by introduction of penalty term [12]. The principle of BLF is to force the constrained state away from the constraint boundary for achieving the target of state constraint. Unavoidably, a virtual controller produced in recursive process leads to a more conservative design [14]. To alleviate the abovementioned drawbacks, a simple PID controller with current constraint where penalty term is added to control variable directly was proposed in [15]. However, the existence of a PID controller may weaken the antiinterference ability of the system. While SMC has been regarded as the most efficient method for disturbance rejection and robustness properties in mechatronic system [16–18], and it has been applied in PMSM systems successfully.

The SMC method has two main disadvantages [19, 20]. The first obvious shortcoming is asymptotic convergence to equilibrium point caused by linear features of sliding mode surface, in which the convergence speed is determined by the control gain [21]. For overcoming this inherent defect, terminal SMC (TSMC) has been presented to reduce convergence time by introducing the fractional-order nonlinear term, which allows system states to approach to origin within finite time, regardless of the initial state of system [22]. Compared with SMC, the addition of nonlinear function in sliding mode variable is to enhance the convergence speed [23]. Particularly, fast TSMC (FTSMC) scheme is developed for further improving control performance. Another shortcoming that needs to be mentioned is system chattering, which is mainly caused by the discontinuity of control signal (signum function) near sliding mode surface [24]. Many continuous approximate functions (such as saturation function and hyperbolic tangent function) are adopted to alleviate the influence of discontinuous term and reduce chattering, which are at the expense of certain system performance [25].

To overcome the abovementioned problems, inspired by interior point method [26], a novel FTSMC-based controller with current constraint for noncascade model in PMSM system is designed. In this design, penalty function is employed in control action directly. The contributions of the paper are summarized as follows: (1) An FTSMC-type sliding mode variable is adopted to guarantee evolution curve to have finite-time convergence performance, and scheme with improved reaching law is employed to further achieve faster convergence performance and chattering reduction. (2) By adopting the idea of interior point method, we construct the penalty function directly in the control variable to make the control system with state constraints an unconstrained system. To the best of our knowledge, it is the first time that the penalty function combined with sliding mode variable is introduced to constrain current in a PMSM system; more importantly, dynamic performance of the controlled system is preserved. (3) The stability proof of noncascade PMSM system is given

in detail, rather than giving the stability of inner and outer loop in cascade structure, respectively.

The structure of the paper is designed as follows. In Section 2, the noncascade model and structure of the PMSM is illustrated in detail. A new reaching law-based FTSMC-type controller with current constraint is developed in Section 3. Section 4 provides lots of simulations. Finally, the concluding results are shown in Section 5.

## 2. A second-order noncascade model for speed regulation system of PMSM

The mathematical model of a surface-mounted PMSM can be formulated as [27]:

$$\begin{cases} i'_d = \frac{u_d}{L_d} - \frac{R_s}{L_d}i_d - \omega p_n i_q \\ i'_q = \frac{u_q}{L_q} - \frac{R_s}{L_q}i_q - \omega p_n i_d - \frac{p_n \Psi_f}{L_q} \omega \\ \frac{d\omega}{dt} = \frac{3p_n i_q \Psi_f}{2J} - \frac{T_L}{J} - \frac{B}{J} \omega \end{cases} \quad (1)$$

where  $u_d$  and  $u_q$  are the stator voltages of d-axis and q-axis;  $i_d$  and  $i_q$  are the stator currents of d-axis and q-axis;  $\omega$  and  $p_n$  are the angular velocity and number of poles pairs;  $L_d$  and  $L_q$  are stator inductance of d-axis and q-axis, and  $L_d = L_q = L$ ;  $R_s$  is the stator resistance;  $\Psi_f$ ,  $T_L$ ,  $J$ , and  $B$  are the rotor flux linkage, load torque, rotor inertia, and viscous friction coefficient, respectively. From system (1), the dynamics constraint of the PMSM model between  $\omega$  and  $i_q$  is:

$$\frac{d\omega}{dt} = \frac{3p_n i_q \Psi_f}{2J} - \frac{T_L}{J} - \frac{B}{J} \omega \quad (2)$$

Taking the derivative of formula (2), we can obtain:

$$\ddot{\omega} = \frac{3p_n \Psi_f}{2J} \dot{i}_q - \frac{\dot{T}_L}{J} - \frac{B}{J} \dot{\omega} \quad (3)$$

In order to effectively realize decoupling control of stator current and angular velocity, the input signal of d-axis controller is set as  $i_d^* = 0$ . In such case, substituting formula (1) into (3), a noncascade PMSM model is shown as:

$$\begin{cases} \ddot{\omega} = -f(\dot{\omega}, \omega) - \frac{b}{L} u_q - d(t) \\ f(\dot{\omega}, \omega) = \left( \frac{B}{J} - \frac{R_s}{J} \right) \dot{\omega} - \left( \frac{b \Psi_f p_n}{L} + \frac{R_s B}{L J} \right) \omega \\ d(t) = -b \omega p_n i_d - \frac{\dot{T}_L}{J} - \frac{R_s T_L}{L J} \\ s.t. \quad |i_q| \leq c_m \end{cases} \quad (4)$$

where  $b = 3p_n \Psi_f / 2J$ , and  $u_q$  is direct control variable for noncascade control structure. The structure of noncascade control for PMSM is shown in Figure 1, the control target is to realize control of speed regulation; meanwhile, the q-axis current is restricted in safety boundary simultaneously, i.e.  $|i_q| \leq c_m$ . In noncascade

control, overcurrent protection cannot simply restrict current by governing the input signals of q-axis current controller, since current controller in control channel is merged into speed controller.

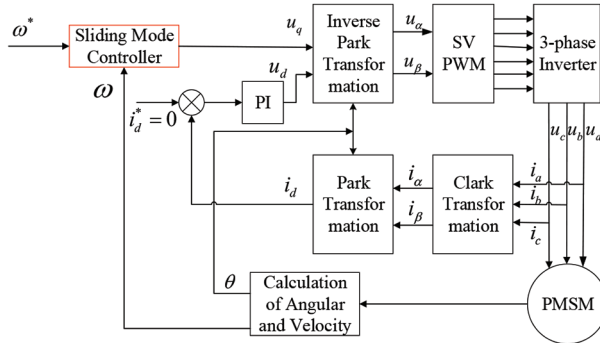


Figure 1. The structure of noncascade control for PMSM.

**Remark 1**  $c_m$  is the threshold of maximum current, which is always two to three times rated current of PMSM.

Defining  $x_1 = \omega^* - \omega$ , where  $\omega^*$  is target value of speed regulation, and  $x_2 = \dot{x}_1$ . The second-order noncascade model is formulated:

$$\begin{cases} \dot{x}_1 = x_2 \\ \dot{x}_2 = \ddot{\omega}^* - \frac{b}{L}u_q + f(\dot{\omega}, \omega) + d(t) \\ s.t. |i_q| \leq c_m \end{cases} \quad (5)$$

where  $d(t)$  is the bounded disturbances;  $u_q$  is the direct control variable that needed to be designed. In the process of controller design, the current must be less than the maximum allowable current to meet the conditions  $|i_q| \leq c_m$ .

### 3. Controller design

#### 3.1. Fast terminal sliding mode controller design

To provide a finite-time convergence performance, FTSMC-based surface is given:

$$s = \lambda_1 |x_1|^{\alpha_1} \text{sign}(x_1) + \lambda_2 x_1 + x_2 \quad (6)$$

where  $\lambda_1 \geq 0$ ,  $\lambda_2 \geq 0$ ;  $\alpha_1 = q/p < 1$ ;  $p$  and  $q$  are positive odd integers. Once reaching the sliding mode surface, the system dynamics can be simplified as a stable equation which is independent of the system disturbances. In such case, the system is rewritten as ordinary differential equation (ODE):

$$\lambda_1 |x_1|^{\alpha_1} \text{sign}(x_1) + \lambda_2 x_1 + x_2 = 0 \quad (7)$$

When the system state is far away from the origin, the system equation simplifies as  $\dot{x}_2 = -\lambda_1 |x_1|^{\alpha_1} \text{sign}(x_1)$ , which has the same performance as TSMC. When system state approaches zero, the dynamics can be approximated to  $\dot{x}_2 = -\lambda_2 x_1$ , the state of system shows exponential convergence, which drives the tracking error

converge to the origin quickly. In order to intuitively display the convergence performance of FTSMC, the phase trajectory of FTSMC is given in Figure 2, in which the initial state is (62.8, 0). Obviously, the phase trajectory converges to the origin with faster speed, which is consistent with the above analysis. According to the ODE (7), analytically, then the convergence time of the system state is calculated as [28]:

$$t_c = \frac{1}{\lambda_2 \alpha_1} \left( \ln (\lambda_2 x_1(0)^{\alpha_1} + \lambda_1) - \ln \lambda_1 \right) \tag{8}$$

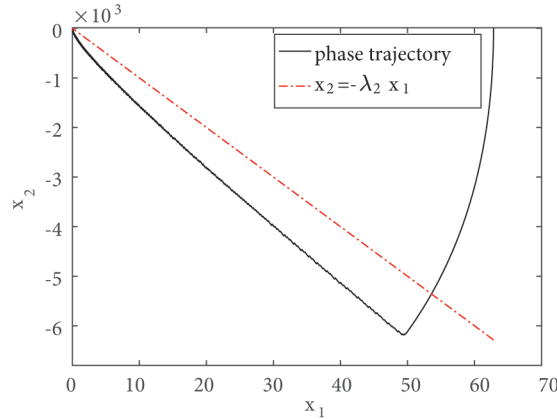


Figure 2. The phase trajectory of FTSMC.

### 3.2. Proposal of improved reaching law

Next, for the purpose of improving reaching speed and weakening chattering phenomenon, the improved reaching law (IRL) is designed as:

$$\dot{s} = -k_1 \tanh(l_1 s) - k_2 s (e^{l_2 |s|} + c) \tag{9}$$

where  $\tanh(s) = (e^s - e^{-s}) / (e^s + e^{-s})$ ;  $k_1, k_2, l_1, l_2 \geq 0$ ;  $c \geq -1$  is the critical parameter to eliminate the effect of second term. One outstanding advantage of the proposed IRL is its capability to vary the reaching time which depends on the position of the state variable. The farther the distance is, the faster the reaching speed is, and vice versa.

In order to more intuitively express the effects of two nonlinear terms in IRL, the changing rate of the two terms are needed to be analyzed. Figure 3 shows the changing rate of two terms when  $s$  belongs to  $[-1, 1]$ . It can be seen that the second term with power term plays a major role of reducing reaching time, when  $s$  is far away from zero. When  $s \rightarrow 0$ , the changing rate mainly depends on the hyperbolic tangent term. Especially, the existence of  $\tanh(l_1 s)$  provides an approximately linear characteristic to approach zero, which weakens the discontinuity of signum function and realizes 'soft' switch control. In this way, the chattering phenomenon is reduced.

The process of improved reaching law shows: 1) Firstly, the original state  $s_0 \neq 0$  and is large, due to the initial position of system state; 2) Then, the second term  $-k_2 s (e^{l_2 |s|} + c)$  is able to force  $s$  to approach zero with faster reaching speed compared with  $-k_1 s$ , until approaching to bound layer; 3) In addition, selecting the proper parameters  $l_2$  and  $c$  to guarantee  $-k_2 s (e^{l_2 |s|} + c) \approx 0$ , when  $s \rightarrow 0$ . In this way, the impact of

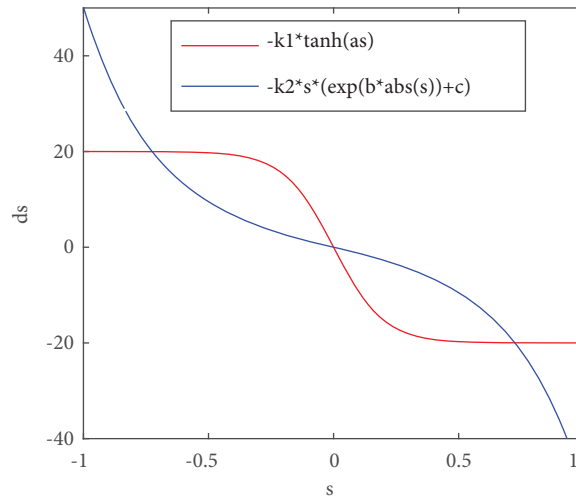


**Figure 3.** The changing rate of two items in the proposed reaching law.

the second item is eliminated to some certain. 4) Finally, the first term  $-k_1 \tanh(l_1 s)$  plays the main role of providing an approximately linear characteristic to approach zero and reducing chattering.

**Remark 2** *The proposal of reaching law is used to achieve fast convergence and chattering reduction. The selection criteria of parameters in reaching law are: (I) the gains  $k_1$  and  $l_1$  should be large enough to handle the lumped disturbance  $d(t)$  in (5) and obtain smaller convergence region; (II) the choice of  $c$  is as close to  $-1$  as possible to eliminate the effect of the second term, when  $s$  approaches zero. (III) the gain  $k_2$  and  $l_2$  should have large positive values to guarantee reaching speed.*

### 3.3. The construction of penalty term based on interior point method

Since q-axis current becomes the internal state of noncascade structure in PMSM control system, in order to realize current constraint, the penalty function method is introduced. The main purpose of the penalty function is to prevent the constrained state from leaving the constraint bounds, because the initial constrained states are within constraint boundary. In this paper, the basic idea of the penalty function method is that constraint conditions and control variable are combined to construct a new control variable. In such case, a control system with state constraints becomes an unconstrained system. In this section, we mainly discuss the construction of penalty term.

For constraining the q-axis current, we introduce the idea of interior point method [26] in optimization theory. Considering the constrained condition  $|i_q| \leq c_m$ , the penalty term is constructed as follows:

$$f_{pt} = \frac{k}{(c_m - |i_q|)^2 s} \tag{10}$$

where  $f_{pt}$  is penalty term. The penalty factor  $k$  is a positive constant representing the penalty force.  $s$  is sliding mode variable. When the q-axis current approaches current threshold  $\pm c_m$ , the penalty term tends to be infinite, the existence of the penalty function in the control variable is to guide the constrained state to move towards the trend of satisfied condition, the q-axis current will be constrained in safe range. While sliding the

mode variable  $s \rightarrow 0$ , the penalty term has only slight impact on control action, the impact on q-axis current will be ignored. More importantly, dynamic performance is preserved by employing the FTSMC-type controller with penalty function, since maximum current is allowed to provide high torque. In this way, the problem of dynamic performance and current constraint is well balanced, and the contradiction between performance and current constraint is solved.

**Remark 3** *First, the existence of sliding mode variable  $s$  in penalty term is applied to guarantee the stability of the whole system. In addition, it provides a convenient way to balance current constraint and dynamic performance. Finally, the penalty factor  $k$  should be carefully chosen by considering the chattering phenomenon in PMSM system.*

### 3.4. The structure design of FTSMC-based controller with current constraint

The controller structure with current constraint is designed in Figure 4. The control variable contains equivalent control, switching control, and penalty function. Especially, the addition of penalty function makes the state constrained system become an unconstrained control system. The whole controller is designed as:

$$u_q = u_{eq} - u_{sw} - u_{PF} \tag{11}$$

$$u_{eq} = \frac{L}{b} \left( \ddot{\omega}^* + f(\dot{\omega}, \omega) + \lambda_1 \alpha_1 |x_1|^{\alpha_1-1} x_2 + \lambda_2 x_2 \right) \tag{12}$$

$$u_{sw} = -\frac{L}{b} \left( k_1 \tanh(l_1 s) + k_2 s \left( e^{l_2 |s|} + c \right) \right) \tag{13}$$

$$u_{PF} = -\frac{L}{b} f_{pt} = -\frac{L}{b} \frac{k}{(c_m - |i_q|)^2} s \tag{14}$$

where  $u_{PF}$  is the penalty function constructed by penalty term (10). The penalty function plays a role of current constraint during the phase of start-up, because the current in other phases will not exceed the maximum allowable current. The results are analyzed in detail in Section 4.

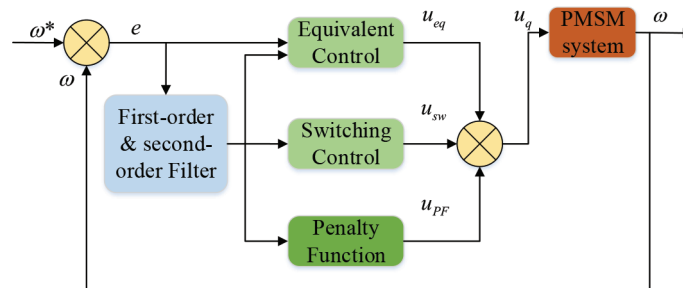


Figure 4. Controller structure with penalty function.

The following gives the convergence proof of new reaching law-based FTSMC-type controller with current constraint for whole PMSM.

**Assumption 1** The lumped disturbances  $d(t)$  is bounded, and a strictly positive constant  $l \geq 0$  exists to satisfy  $0 \leq |d(t)| \leq l$ .

**Theorem 1** If the Assumption 1 is satisfied, the sliding mode variable can converge to region  $(1/l_1) \operatorname{atanh}(l/k_1)$  in finite time by adopting the control law (11). Furthermore, the system states  $x_1$  and  $x_2$  will converge to the origin.

**Proof** Defining the Lyapunov function  $V = 0.5s^2$ , we can obtain by derivation  $\dot{V} = s\dot{s}$ :

$$\begin{aligned} \dot{V} &= s \left( \lambda_1 \alpha_1 |x_1|^{\alpha_1-1} x_2 + \lambda_2 x_2 + \dot{x}_2 \right) \\ &= s \left( \lambda_1 \alpha_1 |x_1|^{\alpha_1-1} x_2 + \lambda_2 x_2 + \ddot{\omega}^* - \frac{b}{L} u + f(\dot{\omega}, \omega) + d(t) \right) \\ &= s \left( k_1 \tanh(l_1 s) + k_2 s \left( e^{l_2 |s|} + c \right) + d(t) - \frac{k}{(c_m - |i_q|)^2} s \right) \\ &\leq k_1 \tanh(l_1 s) s - k_2 s^2 \left( e^{l_2 |s|} + c \right) + l |s| - \frac{k}{(c_m - |i_q|)^2} s^2 \\ &= - \left( \frac{k}{(c_m - |i_q|)^2} + k_2 \left( e^{l_2 |s|} + c \right) \right) s^2 - \left( k_1 \tanh(l_1 |s|) - l \right) |s| \end{aligned} \tag{15}$$

Since  $c > -1$ ,  $k_2 s \left( e^{l_2 |s|} + c \right) > 0$ ,  $k / (c_m - |i_q|)^2 > 0$ . Thus, it can be simplified as:

$$\dot{V} < - \left( k_1 \tanh(l_1 |s|) - l \right) |s| \tag{16}$$

The following condition is satisfied to realize the stability of the closed-loop system:

$$k_1 \tanh(l_1 |s|) - l > 0 \tag{17}$$

and it leads to

$$|s| \geq (1/l_1) \operatorname{atanh}(l/k_1) \tag{18}$$

It is demonstrated that  $\dot{V} < 0$  is satisfied, when sliding mode variable satisfies  $|s| \geq 1/(1/l_1) \operatorname{atanh}(l/k_1)$ . Then  $s$  will converge to the region of  $(1/l_1) \operatorname{atanh}(l/k_1)$  from the initial state. According to the Lyapunov stability theory, it is concluded that  $s$  reaches the region  $|s| \leq (1/l_1) \operatorname{atanh}(l/k_1)$  with a faster convergence rate. In addition, the  $x_1$  and  $x_2$  converge to the origin in finite time.  $\square$

#### 4. Simulation and results analysis

Lots of simulations are provided to validate the superiority and effectiveness of FTSMC-based controller with current constraint from four aspects: (1) The effectiveness validation of penalty function; (2) The comparative simulation under different penalty factor  $k$ ; (3) The improvement of improved reaching law: reaching rate and chattering reduction; (4) The superiority validation compared with other SMC schemes. It should be mentioned that the limit of control signals  $u_q$  are set as 162 (it is calculated as  $311 * 0.9 * \sqrt{1/3}$ ) to guarantee fair comparison. The target speed and load torque are set as  $\omega^* = 600 \text{ r/min}$ ,  $T_L = 3 \text{ N.m}$   $t \geq 0.2 \text{ s}$ . Table 1 shows main parameters of the PMSM.

**Table 1.** Main parameters of the PMSM.

Rated power $P$	2 kW	Stator induction $L$	8.5 mH
Rated current $I$	5.4 A	Viscous coefficient $B$	0.002 Nms/rad
Flux linkage $\Psi_f$	0.17 Wb	Pole pairs $p_n$	2
Rotor inertia $J$	3 kgm <sup>2</sup>	Stator resistance $R_s$	1.32 $\Omega$

#### 4.1. The effectiveness validation of penalty function

The FTSMC-based controller with penalty function ( $k = 10$ ) and FTSMC-based controller ( $k = 0$ ) in noncascade structure are compared to validate effectiveness of penalty function, in which other controller parameters are the same. Table 2 shows the parameters of the FTSMC-type controller with current constraint.

**Table 2.** The controller parameters.

Sliding mode variable	$\lambda_1$	180	IRL parameters	$k_1$	85,000
	$\lambda_2$	100		$k_2$	10,000
	$\alpha_1$	3/5		$l_1$	0.07
PI controller of d-axis	$k_p$	660	$c$	-0.9	
	$k_i$	42.6	$l_2$	0.02	

Figures 5a–5d show response curve of speed  $\omega$ , q-axis current  $i_q$ , phase trajectory, and control variable  $u_q$ . As shown in Figure 5, the existence of penalty function realizes current constraint, and it guarantees the PMSM to start up within maximum current 15 A under start-up phase. While the FTSMC-based controller could achieve higher speed with large current, q-axis current is far larger than the maximum allowable current  $c_m$ , and it may damage the hardware circuit.

During the phase of sudden load disturbance, the q-axis current does not exceed the threshold value of the maximum allowable current, penalty function performs as a small proportional term to accelerate the convergence speed. The results reveal that the speed converges to the target value in a shorter time compared with the FTSMC-based controller. When the control system of PMSM enters the steady state, sliding mode variable converges to bounded region; therefore, penalty function has a slight influence on the dynamic performance, the chattering variation of q-axis current and control variable is not obvious, since influence of penalty function on the control variable mainly depends on the convergence bound of sliding mode variable. In this way, the tradeoff of dynamic performance and current constraint is made by selecting the penalty factor properly.

Furthermore, the phase trajectory of FTSMC and FTMSC+PF schemes have been compared. Obviously, the penalty function has the ability of constraining current. The constraint principle of q-axis current can be expressed as  $\dot{\omega} = 3p_n i_q \Psi_f / 2J - T_L / J - B\omega / J$ . In addition,  $x_2 = \dot{\omega}^* - \dot{\omega}$ . Therefore, when the current is constrained, the state  $x_2$  is also constrained.

#### 4.2. The comparative simulation under different penalty factors $k$

In this section, three different values of  $k$  are selected to verify the effect of the penalty force on PMSM system, where the same controller parameters are chosen to guarantee fair comparison. Response curve of speed  $\omega$ , q-axis current  $i_q$ , d-axis current  $i_d$ , and control variable  $u_q$  are shown in Figure 6.

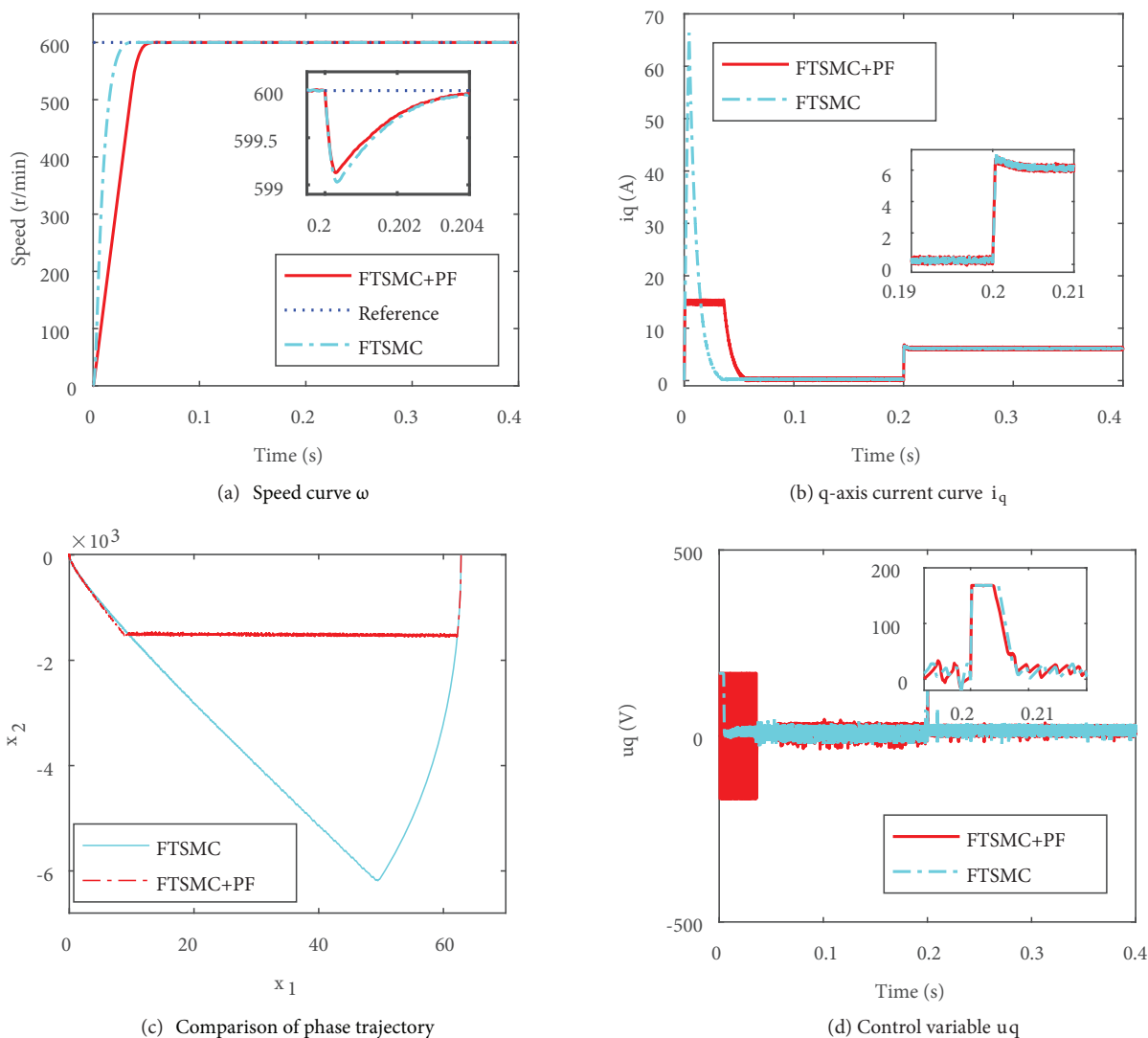


**Figure 5.** The response curve of FTSMC controller and FTSMC controller with current constraint

According to Theorem 1, a strictly positive constant  $k$  is needed to realize the stability of PMSM and constraining current. As is shown, smaller penalty factor ( $k = 5$ ) may lead to the failure of current constraint; other two groups ( $k \geq 10$ ) have function of current constraint in the PMSM system. However, during the start-up phase, the penalty function plays an important role to constrain current in control variable; as a consequence, the increase of penalty factor inevitably results in the increase of chattering in control variable  $u_q$ , it further leads to the torque ripple of PMSM. It also brings burden to hardware.

In addition, the increase of penalty factor also increases the chattering of two currents. It is worth emphasizing that the penalty function cannot improve the convergence speed, because the PMSM starts at the maximum current. In the stage of sudden load disturbance, the increase of penalty factor leads the faster response of speed, since the penalty function plays the role of proportion term. Larger penalty factor determines larger proportional term, and the larger proportion term will result in the faster response of current. Therefore, faster response of current provides higher torque to reduce convergence time inevitably.

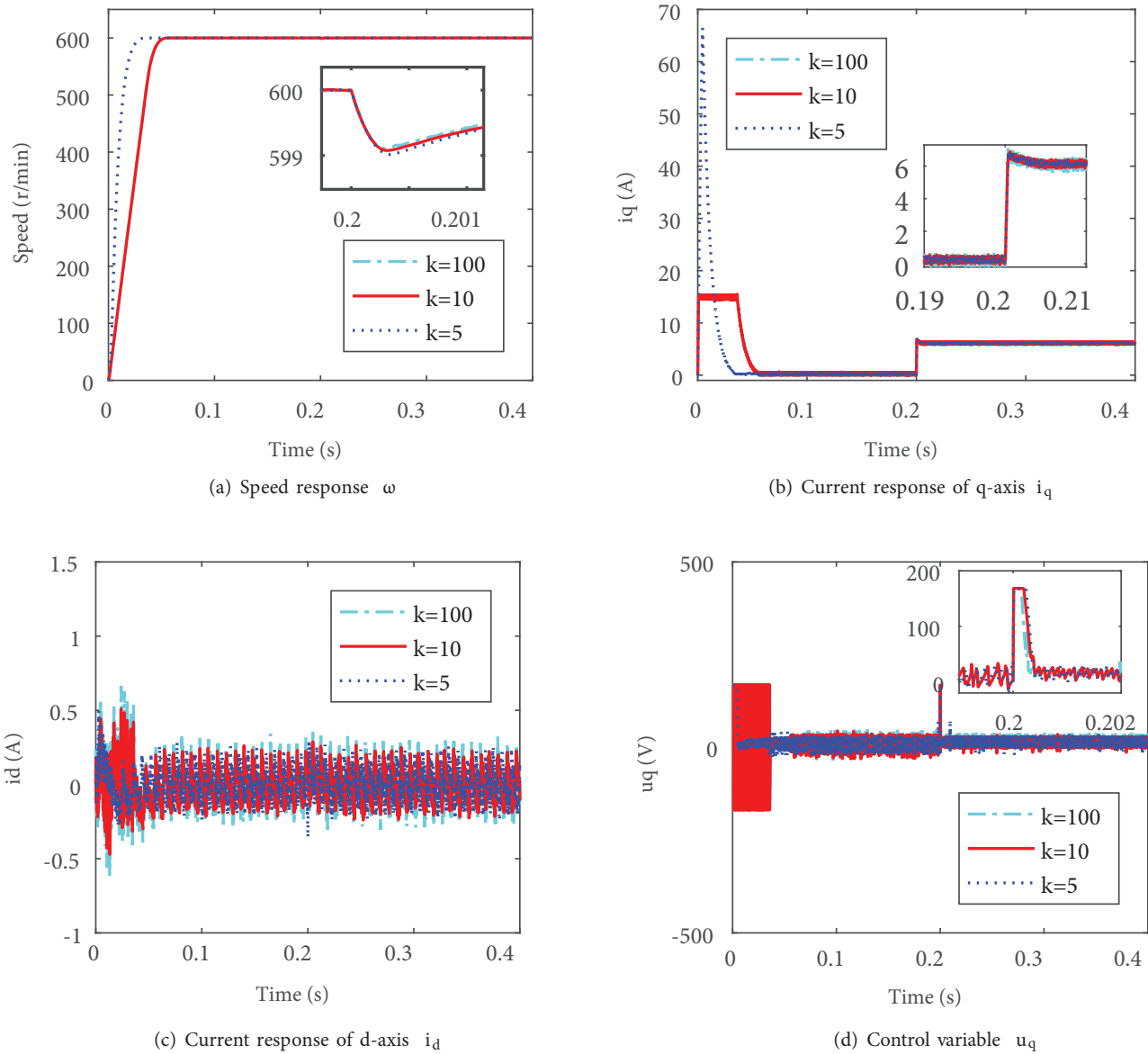


**Figure 6.** The response curve of the proposed controller under different penalty factors.

When the speed regulation system enters into the steady state, the  $s$  keeps in the convergence region  $(1/l_1) \operatorname{atanh}(l/k_1)$ , so the impact of penalty factor on the dynamic performance depends on convergence region. Figure 6 demonstrates that the system chattering increases along with the increase of penalty factor, which is the same as the simulation analysis. Therefore, the penalty factor  $k$  should be selected properly by taking the system chattering into account.

### 4.3. The superiority validation of IRL

For validating the superiority of the proposed reaching law, the constant plus proportional rate reaching law (CPPRL:  $\dot{s} = -k_3 \operatorname{sign}(s) - k_4 s$ ) and hyperbolic tangent reaching law (HTRL:  $\dot{s} = -k_5 \tanh(l_3 s)$ ) are compared. Table 3 expresses the parameters of two reaching laws. Evolution trajectory of speed  $\omega$ , q-axis current  $i_q$ , control variable  $u_q$ , and sliding mode variable  $s$  are shown in Figure 7.

**Table 3.** The parameters in different reaching laws.

CPPRL parameters	$k_3$	100,000	HTRL parameters	$k_5$	120,000
	$k_4$	130,00		$l_3$	0.07

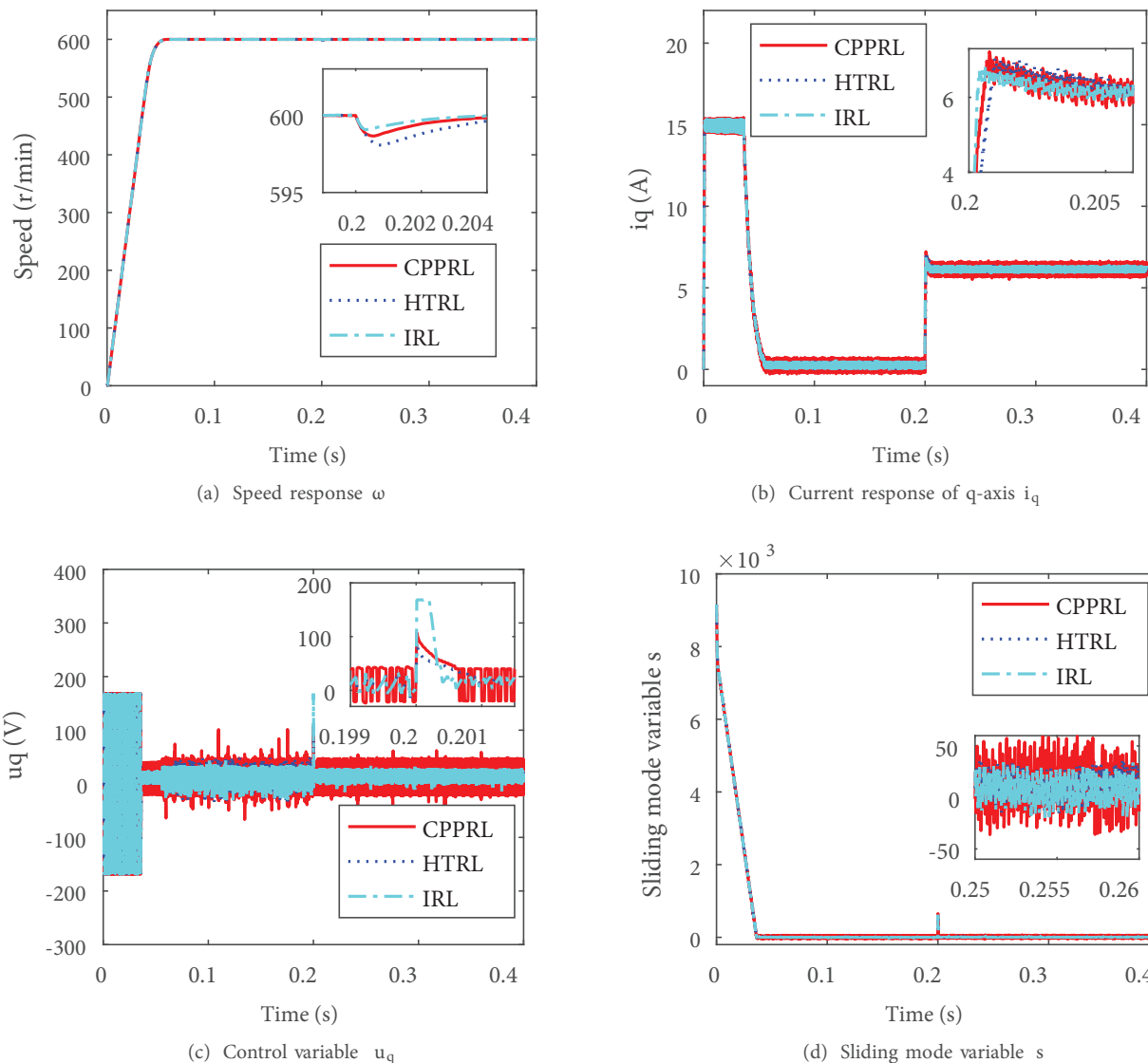


**Figure 7.** The response curve of controller with different reaching law.

During the start-up phase, the penalty function plays a major role, permanent-magnet synchronous motor starts at the maximum allowable current. Therefore, the chattering reduction and faster convergence performance are not prominent. During the phase of sudden load disturbance, the proposed IRL has a great advantage in reducing chattering and faster convergence rate compared with the CPPRL, which is consistent with our analysis. Furthermore, the IRL has faster reaching rate compared with HTRL, since conservative parameters are required to take account of reaching speed and chattering in hyperbolic tangent reaching law. The system chattering mainly relies on signum function term or hyperbolic tangent function term under steady-

state phase; consequently, HTRL and IRL have significant chattering reduction compared with CPPRL; in the same way, HTRL and IRL have similar performance. From the results, it can be concluded that the improved reaching law performs satisfactorily and effectively.

**4.4. The superiority validation compared with other SMC schemes**

In this section, we mainly verify the convergence performance of the FTSMC method compared with SMC ( $s_{SMC} = x_2 + 180x_1$ ) and TSMC ( $s_{TSMC} = x_2 + 180x_1^{3/5}$ ) algorithm. For convergence validation (the same controller parameters are selected to have fair comparison), the speed response  $\omega$ , q-axis current  $i_q$ , and phase trajectory of three schemes are shown in Figure 8. In the start-up phase, all three methods can have higher start-up speed with the maximum current. When entering the convergence phase, the FTSMC+PF approach can provide higher starting current to ensure the start-up speed, while the other two methods have relatively small start-up currents, which inevitably leads to longer convergence time. Obviously, the proposed FTSMC+PF scheme has a better convergence rate compared with TSMC+PF and SMC+PF methods, which is consistent with our above analysis.

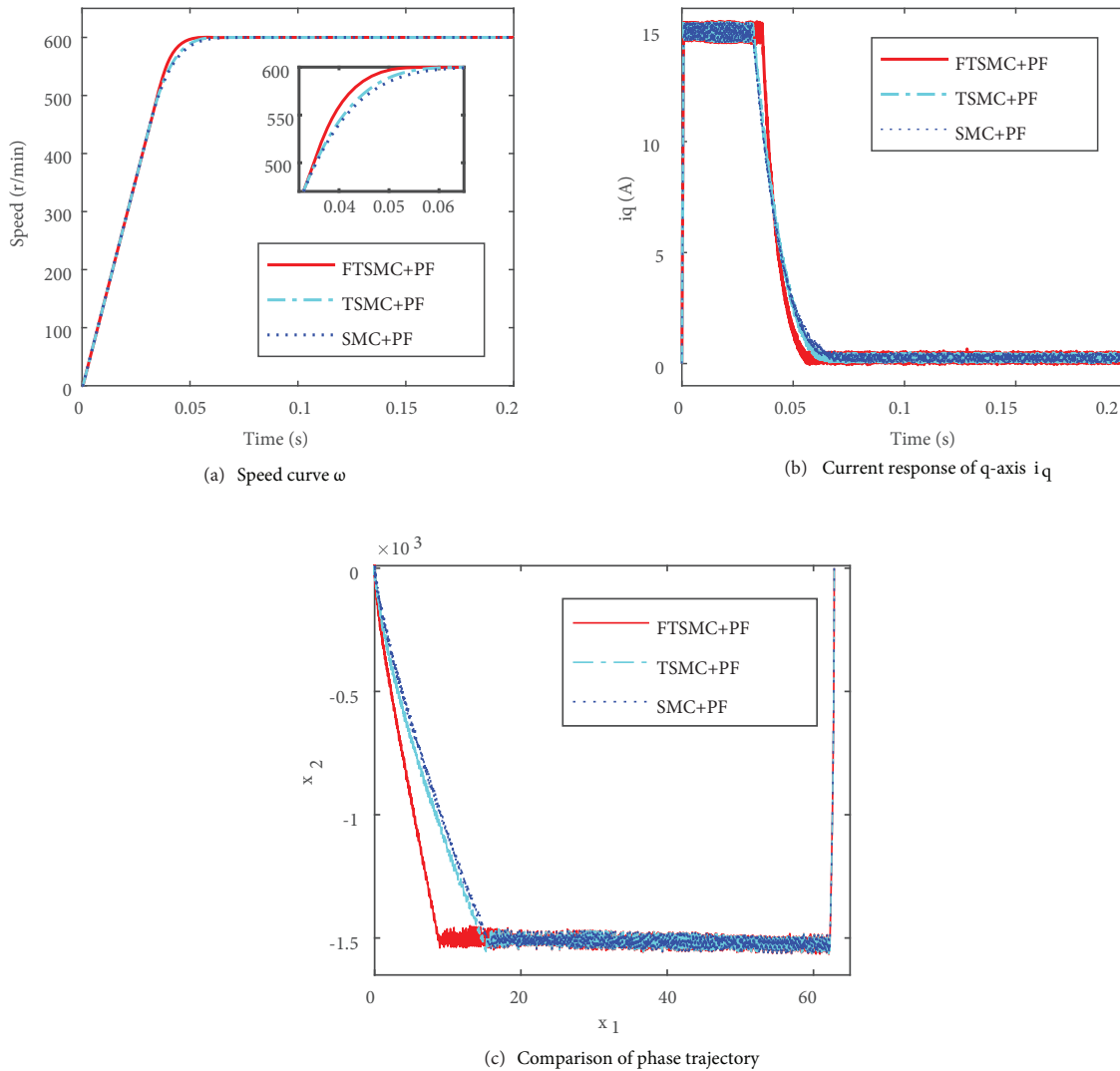


**Figure 8.** The response curve of controller with different SMC methods.

## 5. Conclusions

In this paper, the balance problem between overlarge-current protection and dynamic performance under noncascade structure in PMSM system has been discussed. At first, an improved reaching law-based fast terminal sliding mode controller is developed for noncascade structure in PMSM system to guarantee the fast convergence and chattering reduction. Then, the penalty function established in control action is designed for constraining current with the aid of the idea of interior point method. In such case, the control system with state constraint becomes the unconstrained system. In addition, the existence of sliding mode variable in penalty function keeps the dynamic performance of PMSM system without violating constrained condition. Different simulations have been carried out for demonstrating excellent performance. More importantly, the proposal of penalty function builds the bridge between control problem with state constraint and constrained optimization system.

## References

- [1] Donato DG, Scelba G, Pulvirenti M, Scarcella G, Capponi FG. Low-cost, high-resolution, fault-robust position and speed estimation for PMSM drives operating in safety-critical systems. *IEEE Transactions on Power Electronics* 2019; 34 (1): 550-564. doi: 10.1109/TPEL.2018.2820042
- [2] Xu W, Jiang Y, Mu C. Novel composite sliding mode control for PMSM drive system based on disturbance observer. *IEEE Transactions on Applied Superconductivity* 2016; 26 (7): 1-5. doi: 10.1109/TASC.2016.2611623
- [3] Li S, Zong K, Liu H. A composite speed controller based on a second-order model of permanent magnet synchronous motor system. *Transactions of the Institute of Measurement and Control* 2011; 33 (5): 522-541. doi: 10.1177/0142331210371814
- [4] Hu Z, Hameyer K. A method of constraint handling for speed-controlled induction machines. *IEEE Transactions on Industrial Electronics* 2016; 63 (7): 4061-4072. doi: 10.1109/TIE.2016.2532843
- [5] Preindl M, Bolognani S. Model predictive direct torque control with finite control set for PMSM drive systems, Part 1: maximum torque per ampere operation. *IEEE transactions on industrial informatics* 2013; 9 (4): 1912-1921. doi: 10.1109/TII.2012.2227265
- [6] Kim SK, Lee KG, Lee KB. Singularity-free adaptive speed tracking control for uncertain permanent magnet synchronous motor. *IEEE Transactions on Power Electronics* 2016; 31 (2): 1692-1701. doi: 10.1109/TPEL.2015.2422790
- [7] Xu W, Junejo AK, Liu Y, Islam MR. Improved continuous fast terminal sliding mode control with extended state observer for speed regulation of PMSM drive system. *IEEE Transactions on Vehicular Technology* 2019; 68 (11): 10465-10476. doi: 10.1109/TVT.2019.2926316
- [8] Yu J, Ma Y, Yu H, Lin C. Reduced-order observer-based adaptive fuzzy tracking control for chaotic permanent magnet synchronous motors. *Neurocomputing* 2016; 214: 201-209. doi: 0.1016/j.neucom.2016.05.088
- [9] Petrovic V, Ortega R, Stankovic AM. Interconnection and damping assignment approach to control of PM synchronous motors. *IEEE Transactions on Control Systems Technology* 2001; 9 (6): 811-820. doi: 10.1109/87.960344
- [10] Fuentes E, Kalise D, Rodriguez J, Kennel RM. Cascade-free predictive speed control for electrical drives. *IEEE Transactions on Industrial Electronics* 2014; 61 (5): 2176-2184. doi: 10.1109/TIE.2013.2272280
- [11] Sun Z, Guo T, Yan Y, Wang X, Li S. A composite current-constrained control for permanent magnet synchronous motor with time-varying disturbance. *Advances in Mechanical Engineering* 2017; 9(9): 168781401772869. doi: 10.1177/1687814017728691
- [12] Liu Y, Tong S. Barrier Lyapunov Functions-based adaptive control for a class of nonlinear pure-feedback systems with full state constraints. *Automatica* 2016, 64 (C): 70-75. doi: 10.1016/j.automatica.2015.10.034

- [13] Mwasilu F, Nguyen HT, Choi HH, Jung JW. Finite set model predictive control of interior PM synchronous motor drives with an external disturbance rejection technique. *IEEE/ASME Transactions on Mechatronics* 2016; 22 (2): 762-773. doi: 10.1109/TMECH.2016.2632859
- [14] Liu Y, Gong M, Tong S, Chen C, Li D. Adaptive fuzzy output feedback control for a class of nonlinear systems with full state constraints. *IEEE Transactions on Fuzzy Systems* 2018; 26 (5): 2607-2617. doi: 10.1109/TFUZZ.2018.2798577
- [15] Guo T, Sun Z, Wang X, Li S, Zhang K. A simple current-constrained controller for permanent-magnet synchronous motor. *IEEE transactions on industrial informatics* 2019; 15 (3): 1486-1495. doi: 10.1109/TII.2018.2860968
- [16] Zhang X, Sun L, Zhao K, Sun L. Nonlinear speed control for PMSM system using sliding-mode control and disturbance compensation techniques. *IEEE Transactions on Power Electronics* 2013; 28 (3): 1358-1365. doi: 10.1109/TPEL.2012.2206610
- [17] Wang H, Chang L, Tian Y. Extended state observer-based backstepping fast terminal sliding mode control for active suspension vibration. *Journal of Vibration and Control* 2020; 10: 1077546320959521. doi: 10.1177/1077546320959521
- [18] Asl SBF, Moosapour SS. Adaptive backstepping fast terminal sliding mode controller design for ducted fan engine of thrust-vectoring aircraft. *Aerospace Science and Technology* 2017; 71: 521-529. doi: 10.1016/j.ast.2017.10.001
- [19] Jiang J, Zhou X, Zhao W, Li W, Zhang W. A fast integral sliding mode controller with an extended state observer for position control of permanent magnet synchronous motor servo systems. *Frontiers of Information Technology and Electronic Engineering* 2020; 21(8): 1239-1250. doi: 10.1631/FITEE.1900298
- [20] Köse E, Kizmaz H, Abaci K, Aksoy S. Control of SVC based on the sliding mode control method. *Turkish Journal of Electrical Engineering and Computer Sciences* 2020; 22 (3): 605-619. doi: 10.3906/elk-1209-8
- [21] Zhihong M, Yu X. Terminal sliding mode control of MIMO linear systems. *IEEE Transactions on Circuits and Systems I Fundamental Theory and Applications* 1997; 44 (11): 1065-1070. doi: 10.1109/81.641769
- [22] Van M. An enhanced robust fault tolerant control based on an adaptive fuzzy PID-nonsingular fast terminal sliding mode control for uncertain nonlinear systems. *IEEE/ASME Transactions on Mechatronics* 2018; 23 (3): 1362-1371. doi: 10.1109/TMECH.2018.2812244
- [23] Liang X, Fei J, Wang Z. Robust adaptive fractional fast terminal sliding mode controller for microgyroscope. *Complexity* 2020; 2020: 1-18. doi: 10.1155/2020/8542961
- [24] Wang H, Shi L, Man Z, Zheng J, Li S et al. Continuous fast nonsingular terminal sliding mode control of automotive electronic throttle systems using finite-time exact observer. *IEEE Transactions on Industrial Electronics* 2018; 65 (9): 7160-7172. doi: 10.1109/TIE.2018.2795591
- [25] Brahmi B, Laraki MH, Brahmi A, Saad, M, Rahman MH. Improvement of sliding mode controller by using a new adaptive reaching law: Theory and experiment. *ISA transactions* 2020; 97: 261-268. doi: 10.1016/j.isatra.2019.08.010
- [26] Yang X, Bai Y. an adaptive infeasible-interior-point method with the one-norm wide neighborhood for semi-definite programming. *Journal of Scientific Computing* 2019; 78 (3): 1790-1810. doi: 10.1007/s10915-018-0827-2
- [27] Huang Y, Liu Z, Xie Y, Liu Y. Adaptive switching gain sliding mode control for speed regulation in PMSMs. *Turkish Journal of Electrical Engineering and Computer Sciences* 2019; 27 (4): 3208-3218. doi: 10.3906/elk-1703-265
- [28] Solis CU, Clempner JB, Poznyak AS. Fast terminal sliding-mode control with an integral filter applied to a van der pol oscillator. *IEEE Transactions on Industrial Electronics* 2017; 64 (7): 5622-5628. doi: 10.1109/TIE.2017.2677299